

Band structure and thermodynamic properties of He atoms near a graphite surface

William E. Carlos* and Milton W. Cole

Department of Physics, The Pennsylvania State University, University Park, Pennsylvania 16802

(Received 12 September 1979)

The energy-band structure and thermodynamic properties (in the noninteracting limit) of He atoms on graphite are calculated. Bound-state eigenvalues ϵ_n and matrix elements $\langle n|V_{01}|n'\rangle$ obtained in scattering experiments are used as input. The validity of the assumptions used to derive these quantities is verified for self-consistency. The results of these calculations differ from earlier studies in that the binding energies are 15 percent smaller and the corrugation is 50–100 percent larger. The effective mass enhancement m^*/m is 1.06 for ^4He and 1.03 for ^3He . Agreement with adsorption-isotherm determinations of the chemical potential in the limit of low coverage and temperature is remarkably good for both isotopes. These results, which are consistent with our previous analysis of the potential energy $V(\vec{r})$, indicate that band-structure effects cannot be neglected in treating He films on graphite.

I. INTRODUCTION

The subject of physical adsorption has received intensive scrutiny in recent years among workers in fields as diverse as chemical physics and statistical mechanics.¹⁻⁴ One system of particular interest is He on graphite, which exhibits a rich diversity of phases in the submonolayer regime of coverage.³⁻⁶ This paper presents a determination of the energy-band structure of He atoms on graphite. For low coverage and high temperature, this suffices to determine the thermodynamic properties of the film, some of which we compute here. These calculations serve more generally as a basis for understanding effects on the film of both lateral and perpendicular variation of the atom-surface interaction $V(\vec{r})$.

The technique of atomic beam scattering has evolved recently as an effective probe of such interactions.^{7,8} In a recent study^{9,10} (denoted henceforth as CC), we have utilized extensive data^{7,8} for He-graphite scattering to determine plausible forms of $V(\vec{r})$ for this system.¹¹ These potentials are 15–20 percent less attractive and significantly more corrugated than potentials assumed^{4,12,13} prior to the scattering experiments.^{7,8} This difference suggested the desirability of performing a band-structure calculation in order to evaluate the energy spectrum $E(\vec{K})$. Our results are indeed different from those of earlier studies;^{12,13} the first band gap is 56% as wide as the lowest bandwidth, while the earlier work gives this ratio as about 25%. The band structure is still nearly free-particle-like.

As seen below, this calculation is essentially empirical, based almost entirely on the scattering data. The specific quantities used are the eigenvalues ϵ_n of the lateral average potential $V_0(z)$ and the matrix elements of the lowest Fourier component $V_{01}(z)$ of the potential (measured thus

far only for ^4He). The experimental values are summarized in Tables I and II of CC, to which the reader is referred for our notation.¹⁰ In addition to the values measured to date, a refined calculation needs those of the (1) couplings to higher bound states and to continuum solutions of the Hamiltonian, and (2) coupling between bound states by higher Fourier components. Wolfe and Weare¹⁴ have found that the corrections due to coupling to continuum states are much smaller than those due to coupling between bound states; hence we neglect the former. The corrections due to coupling to higher bound states and by higher Fourier components of the potential are both quite small, but we may estimate these from matrix elements computed in CC using the potential $V(\vec{r})$ represented as a sum of anisotropic Yukawa-6 pair interactions. Similarly, the band structure of ^3He on graphite will be calculated using matrix elements computed from the same potential.

Two major questions addressed in this paper are (1) at scattering energies, how much does $E(\vec{K})$ differ from the nearly-free-particle approximation used in deriving the experimental eigenvalues and matrix elements, and (2) what is $E(\vec{K})$ for the most strongly bound states? By examining the first question we obtain an estimate of the corrections to the conventional approximation used to determine the “experimental” eigenvalues and matrix elements. The answers to the second question provide the input for calculating thermodynamic properties of low-coverage He films on graphite. The agreement with experimental data⁵ is remarkably good.

The organization of this paper is as follows. The next section presents our procedure for evaluating the band structure $E(\vec{K})$. Section III discusses the results at high energy, comparable to that of the incident particle in a scattering experiment. Section IV presents low-energy results, which are

used in Sec. V to compute thermodynamic properties. Section VI summarizes our results.

II. GENERAL FORMALISM

The atom-surface interaction $V(\vec{r})$ is periodic with respect of the component $\vec{R} = (x, y)$ parallel to the surface. Letting \vec{G} denote a two-dimensional reciprocal lattice vector, the Hamiltonian is

$$\hat{H} = \hat{T} + V_0(z) + \sum_{\vec{G} \neq 0} V_{\vec{G}}(z) \exp(i\vec{G} \cdot \vec{R}), \quad (1)$$

where \hat{T} is the kinetic energy operator and $\{V_{\vec{G}}(z)\}$ are the Fourier components of the potential at fixed distance z from the outer atomic plane. Our treatment parallels that used to treat electrons in crystals.¹⁵ Here each eigenfunction is labeled by a wave vector \vec{K} appropriate to a two-dimensional Bloch theorem. For a given \vec{K} , the eigenfunctions may be expanded in a complete set of basis functions

$$\psi_{\vec{K}}(\vec{r}) = \sum_{n, \vec{G}} \alpha_{n\vec{G}}(\vec{K}) |n, \vec{G}\rangle, \quad (2a)$$

$$|n, \vec{G}\rangle = \phi_n(z) \exp[i(\vec{K} + \vec{G}) \cdot \vec{R}]. \quad (2b)$$

The functions $\phi_n(z)$ are taken as eigenfunctions with eigenvalue ϵ_n of the one-dimensional Schrödinger equation incorporating the potential $V_0(z)$. Multiplying by $|n', \vec{G}'\rangle$ the Schrödinger equation based on Eqs. (1) and (2) and integrating over a surface unit cell of area a_s yields

$$\sum_{\sigma, \vec{G}'} \left[\left(\epsilon_n + \frac{\hbar^2}{2m} (\vec{K} + \vec{G})^2 \right) \delta_{\vec{G}\vec{G}'} \delta_{n\sigma} + \langle n | V_{\vec{G}-\vec{G}'} | n' \rangle \right] \alpha_{\sigma\vec{G}'}(\vec{K}) = \alpha_{n\vec{G}}(\vec{K}) E(\vec{K}), \quad (3)$$

where

$$\langle n | V_{\vec{G}-\vec{G}'} | n' \rangle = a_s^{-1} \int_{-\infty}^{\infty} \phi_n^*(z) V_{\vec{G}-\vec{G}'}(z) \phi_{n'}(z) dz.$$

The eigenvalues $E(\vec{K})$ of this matrix equation may now be computed almost exclusively from experimental data. That is, the eigenvalues ϵ_n and the matrix elements of V_{01} are measured^{7,8} quantities and only the matrix elements of higher Fourier components are derived from the model potential.^{9,10} This method of computing the band structure is particularly applicable to the problem of He on graphite since the magnitudes of the Fourier components are small (compared to the electronic problem) and decrease rapidly with increasing $|\vec{G}|$.¹⁰ Thus the members of the basis set are good approximations to the eigenfunctions of the full Hamiltonian (except quite close to degeneracy points). For both reasons a relatively small number of terms in the basis set are necessary to ob-

tain an accurate $E(\vec{K})$. For most of this work the 19 smallest \vec{G} ($\vec{G}=0$ and 3 orders of $\vec{G} \neq 0$) values were used for $n=0$ and only $\vec{G}=0$, and the lowest-order nonzero \vec{G} 's were used for $n \neq 0$. In most cases an even smaller basis set suffices, and the large $|\vec{G}|$ matrix elements contribute negligibly.

III. BAND-STRUCTURE EFFECTS AT SCATTERING ENERGY

The nearly-free-atom picture of the resonant state is implicitly assumed when the values of ϵ_n and $\langle n | V_{01} | n' \rangle$ are deduced from the data. This is qualitatively palusible because of the high surface-parallel energy of the resonant state. Here this assumption is validated quantitatively by calculating the band structure of He adsorbed on graphite for energies typical of scattering experiments. Using the band-structure calculation for this purpose is both accurate and convenient, since higher-order corrections and degeneracies are automatically included. Experimentally, the eigenvalues of $V_{\vec{G}}(z)$ are determined by assuming the free-particle (zero-order) description of the resonant state. That is, it is assumed that a resonance occurs when

$$E_i \cong E^0(\vec{K}) = (\hbar^2/2m)(\vec{K} + \vec{G})^2 + \epsilon_n, \quad (4)$$

with E_i the energy of the incident atom and \vec{K} the surface-parallel projection of its wave vector. The resonance actually occurs when the incident energy is equal to one of the eigenvalues $E(\vec{K})$ of the full Hamiltonian. That is,

$$E_i = E(\vec{K}) = (\hbar^2/2m)(\vec{K} + \vec{G})^2 + \epsilon_n + \delta E(\vec{K}), \quad (5)$$

where

$$\delta E(\vec{K}) \equiv E(\vec{K}) - E^0(\vec{K})$$

is the band-structure correction to the free-particle energy and hence to ϵ_n . Similarly, the matrix elements are usually evaluated with degenerate perturbation theory. For example, along the line of degeneracy of the $n(1, 1)$ and $n(0, 1)$ states, the energies are given to first order by

$$E_{\pm}(\vec{K}) = (\hbar^2/2m)(\vec{K} + \vec{G})^2 + \epsilon_n \pm \langle n | V_{01} | n \rangle; \quad (6)$$

that is, the separation between the two bands is assumed to be $2\langle n | V_{01} | n \rangle$. We can then compare the band gap calculated using the full band structure with that predicted by first-order perturbation theory. In this way the band-structure calculation is used to verify the model of the resonant state used in the analysis of experimental data.

Figure 1(a) shows the free atom $E^0(\vec{K})$ obtained from Eq. (4) for \vec{K} along the $[1, 1]$ direction. Also shown (by dots) are eigenvalues $E(\vec{K})$ calculated from Eq. (3). The eigenvalues follow the free-

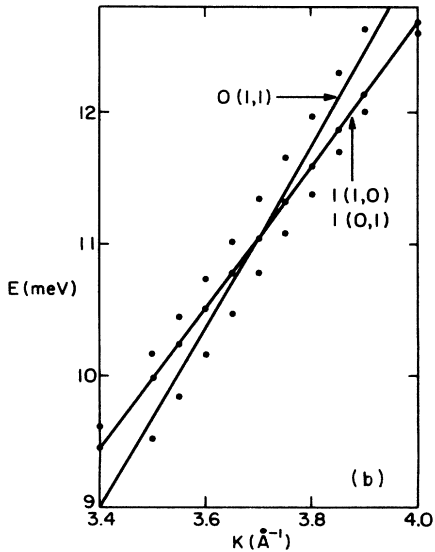
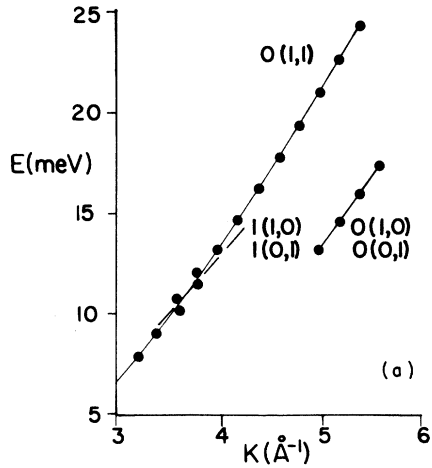


FIG. 1. (a) Energy bands at positive energy for ${}^4\text{He}$ for \vec{K} along $\phi = 0^\circ$, i.e., the $[1, 1]$ direction on graphite. Dots are computed eigenvalues. Curves give the free-particle bands (labeled by n and \vec{G}) which are dashed for the degenerate states $|1, 10\rangle$ and $|1, 01\rangle$. (b) Greatly magnified version showing crossing region. Note that one state follows the unperturbed curve; the other two states are split apart.

atom curves closely except very near points of degeneracy. Far from such regions, the deviations are on the order of ± 0.05 meV, with the sign varying with the azimuthal angle of incidence. The experimentally reported eigenvalues are averages over a range of angles; therefore these deviations may be naively interpreted as scatter in the data.

The portion of the band structure near the crossing of the $0(1, 1)$ free-atom band and the combination of the $1(1, 0)$ and $1(0, 1)$ bands is shown in Fig. 1(b). It is convenient to think of the two de-

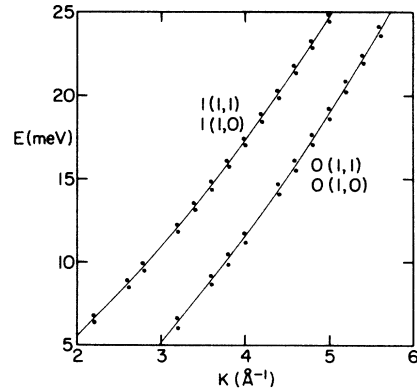


FIG. 2. The $n=0$ and 1 bands for ${}^4\text{He}$ at $\phi = 30^\circ$ (the $[1, 2]$ direction). Each pair is degenerate in the free-particle limit, shown by the curve.

generate $n=1$ bands as symmetric and antisymmetric bands having wave functions given by

$$\psi^\pm = (1/\sqrt{2})(|1, 10\rangle \pm |1, 01\rangle), \quad (7)$$

respectively. The two bands do not couple and have an energy splitting $2\langle 0|V_{11}|0\rangle$ of order 0.02 meV. However, as Chow has pointed out,¹⁶ only the symmetric band will couple to the $0(1, 1)$ band. Therefore, as seen in Fig. 1(b), the antisymmetric band does not mix with the $0(1, 1)$ band. Hence one set of points follows the free-atom curve, while strong mixing of the other two states causes deviation from the free-atom curves.

Figure 2 shows the free atom $E^0(\vec{K})$ for $\phi = 30^\circ$ along with $E(\vec{K})$ calculated with band-structure

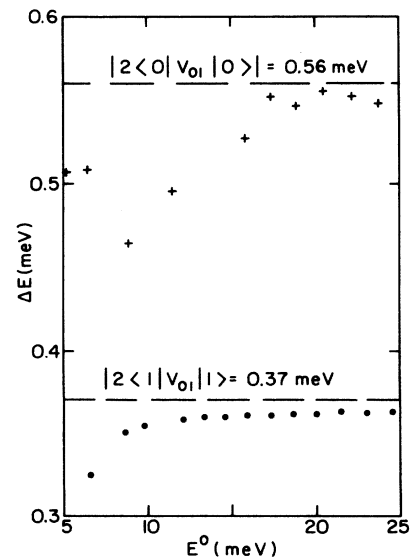


FIG. 3. Energy splitting between the pairs of $n=0$ and 1 states of Fig. 2, plotted as a function of unperturbed energy.

effects. Note the splitting of the states $n(0,1)$ and $n(1,1)$, which are degenerate in zero order. These splittings are plotted for $n=0$ and 1 in Fig. 3. The first-order perturbation theory used to calculate the matrix element from experimental data gives this splitting as $2 \langle n | V_{01} | n \rangle$. As seen in Fig. 3, this is essentially the splitting given by the full band-structure calculation for large E^0 . Because the band-structure effects reduce the splitting so slightly (~ 2 percent near $E = 23$ meV where the data⁸ were taken,) no correction to the experimentally determined matrix elements seems necessary.

Similar calculations were done for ^3He using the matrix elements calculated in CC from the anisotropic Yukawa-6 pair potentials.¹⁰ Since the matrix elements are somewhat smaller and the free-atom energy bands are more widely separated, the band-structure effects are smaller for ^3He than for ^4He . This has a simple interpretation in terms of the larger zero-point vibration of the lighter atom, resulting in smaller overlap with the region of potential corrugation.

IV. BAND STRUCTURE AT LOW ENERGY

The thermodynamic properties of He films for temperature $T < 20$ K depend on the energy spectrum of states within approximately 5 meV of the ground state. Figures 4 and 5 exhibit the spectrum of ^4He and ^3He for this energy range computed by the method of Sec. II. Also shown for comparison is the free-particle spectrum obtained from Eq. (4). Table I summarizes some of the important quantities characterizing these results.

We note that if all matrix elements of Fourier components larger than the smallest $\vec{G} = [0, 1]$ are set to zero, none of the corrections given in Table I change within the precision given there. The band structure at these low energies is almost entirely due to $n=0$ states. If the coupling to the higher states is completely neglected, none of the corrections change by more than 30 percent. At higher energies (~ 6 meV) the weakly perturbed $n=1$ state appears for ^4He (Fig.4). No band can be clearly labeled as due to the first excited state of ^3He since at $K=0$ that free-atom band is nearly degenerate with the $n=0$ bands.

The band structures calculated here are less free-particle-like than those calculated prior to the beam-scattering experiments. For example, the lowest direct gaps at the Q and P points in the Brillouin zone are approximately 50 percent larger than those found previously.^{12,13} The non-negligible effective-mass enhancements of Table I have not been present in earlier work. These differences reflect the larger degree of corruga-

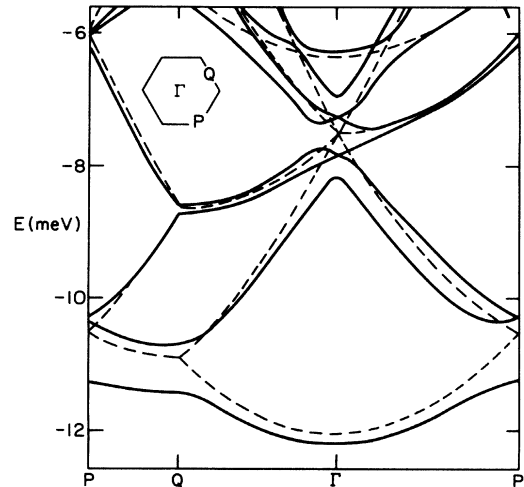


FIG. 4. Band structure of ^4He on graphite (full curve) for \vec{k} along symmetry lines in the two-dimensional Brillouin zone (shown). Dashed curve is the free-particle result, which neglects lateral variation of $V(\vec{r})$.

tion in our potential.¹⁰ For example, the site-to-site potential-energy barrier across the saddle point obtained in CC (Ref.10) is 3 meV, about twice as large as the value present in earlier potentials. As discussed elsewhere,^{9,10} the difference is attributable to previous workers' inadequate choice of He-C pair-potential parameters and omission of anisotropy from the He-C interaction.¹⁷ It is encouraging that the model-independent band structure exhibits a corresponding difference.

V. THERMODYNAMIC PROPERTIES

A very naive approach to the problem of sub-monolayer He films treats the particles as non-

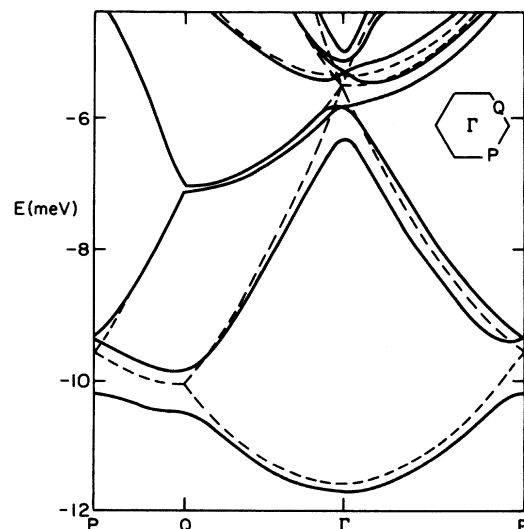


FIG. 5. Same as Fig. 4 for ^3He .

TABLE I. Parameters of band structure. Energies are in meV. Values at specific points are for the lowest bands.

| | | ⁴ He | ³ He |
|---|---------------------------|-----------------|-----------------|
| E_{Γ} | Computed | -12.22 | -11.73 |
| | experimental ^a | -12.27 ± 0.2 | -11.72 ± 0.2 |
| E_P | | -11.26 | -10.23 |
| | | -10.33 | -9.37 |
| E_Q | | -11.43 | -10.52 |
| | | -10.70 | -9.88 |
| $\delta E_{\Gamma} = E_{\Gamma} - \epsilon_0$ | | -0.16 | -0.11 |
| Bandwidth | | 0.96 | 1.48 |
| Band gap (indirect) | | 0.56 | 0.36 |
| m^*/m | | 1.06 | 1.03 |

^a From Elgin *et al.* (Ref. 5).

interacting and moving in two dimensions across a smooth substrate. Several treatments¹⁸ have included interparticle interactions, but no finite-temperature calculation incorporates a realistic three-dimensional He-graphite potential. Here we employ a complementary approach; the potential is authentic, but interactions are omitted. This last deficiency is serious unless the effect of interactions is negligible (low coverage, high temperature) or can be estimated accurately.

We begin by deriving the density of states $N(E)$ from the band structure. The procedure entails evaluating $E_j(\vec{k})$ for a fine mesh of points in the Brillouin zone and counting the number of eigenvalues lying in intervals of width $\Delta E = 0.02$ meV. The results for the two isotopes are shown in Figs. 6 and 7. The “noise” in the output is statistical, arising from the finite number (~100) of eigen-

values in each interval. Also shown in these figures is the free-particle density of states

$$N_0(E) = \frac{m}{2\pi\hbar^2} \sum_n H(E - \epsilon_n), \quad (8)$$

where $H(x)$ is the step function (unity for positive x , zero for negative x). The prefactor preceding the sum is the constant density of states associated with two-dimensional motion for each state n of perpendicular motion. This stepped structure due to onset of successive n bands is also present in $N(E)$. Band-structure effects provide significant differences between the functions $N(E)$ and $N_0(E)$ of Figs. 6 and 7. The clearest discrepancies are, of course, the presence of band gaps and contiguous peaks in $N(E)$. Less dramatic, but quite important, are energy shifts and effective-mass enhancements at the bottom of the band.

The thermodynamic properties of a system of N noninteracting atoms are obtained here from the density of states using the grand canonical ensemble

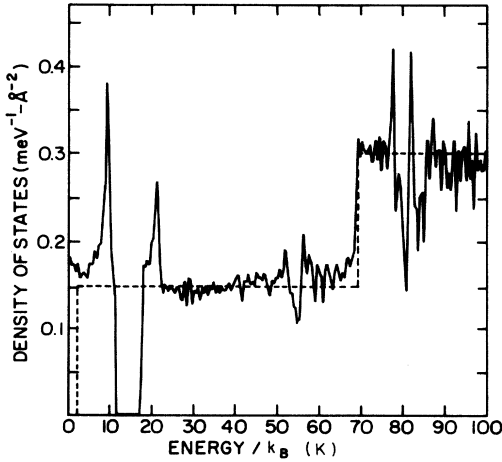


FIG. 6. Density of states for ⁴He (full curve). The ground state represents the zero of the abscissa. Dashed curve is $N_0(E)$, the density of states in the two-dimensional free-particle model.

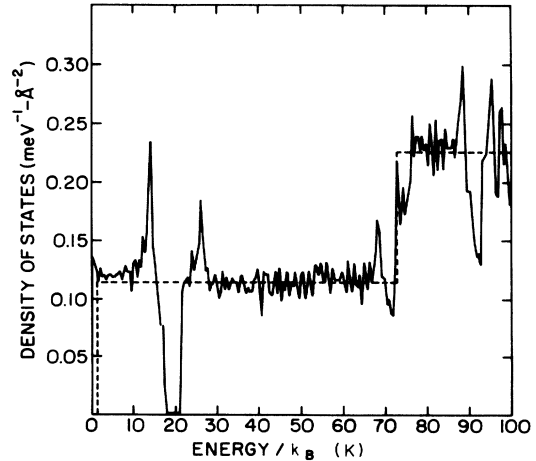


FIG. 7. Same as Fig. 6 for ³He; spin is not included.

ble.¹² The total energy of a system of N atoms is given by

$$U = gA \int_0^\infty N(E) E f(E, T) dE, \quad (9)$$

where A is the total area of the surface, g is the spin degeneracy (1 for ^4He , 2 for ^3He), and

$$f(E, T) = \{\exp[\beta(E - \mu)] \pm 1\}^{-1}.$$

Here $- (+)$ refers to bosons (fermions), $\beta^{-1} = k_B T$, and k_B is Boltzmann's constant. The chemical potential μ is determined by

$$N = gA \int_0^\infty N(E) f(E, T) dE. \quad (10)$$

The isosteric specific heat C/N may then be obtained from

$$C/N = Ak_B \beta^2 (I_2 - I_1^2/I_0)/N, \quad (11)$$

where

$$I_j = g \int_0^\infty N(E) E^j e^{\beta(E - \mu)} f^2(E, T) dE.$$

The chemical potentials for the two isotopes derived from Eq. (10) are shown in Figs. 8 and 9. Results are shown for two coverages, $\theta \equiv N/N_c$, $\theta = 0.2$ and 1.0 , where N_c is that coverage for which there is one He atom for every three hexagons in the basal plane. Only at low coverage or high T are our results reliable in general because the effect of interactions are ignored here. $T=0$ provides an exception, however, because there one can incorporate the known ground-state binding energy.⁵ For ^4He the chemical potential at absolute zero is just E_Γ (-12.22 meV). This com-

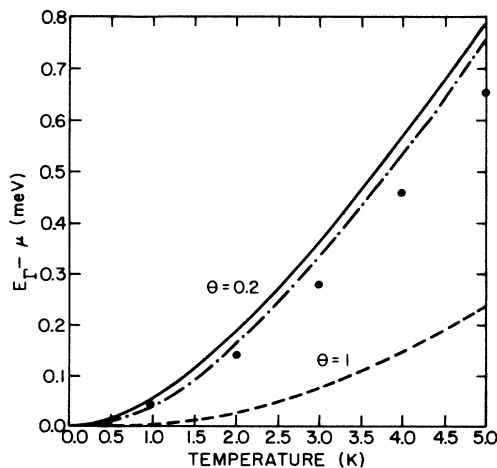


FIG. 8. Chemical potential of ^4He relative to its zero-temperature value computed for relative coverages $\theta = 0.2$ and 1 (full curves). Dash-dot curve represents results in the absence of band-structure effects.

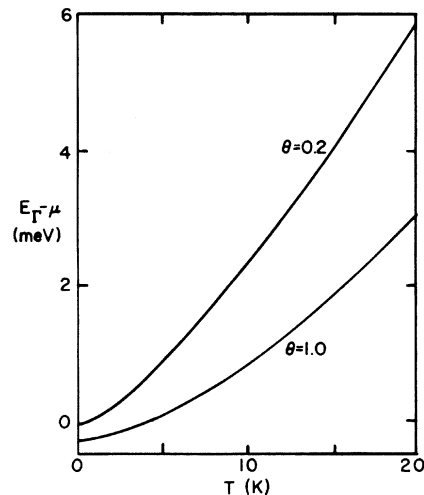


FIG. 9. Chemical potential for ^3He for two coverages.

pares very well with the value derived by Elgin *et al.* from thermodynamic measurements⁵ (-12.27 ± 0.2 meV) after a correction of 0.05 meV is made for the binding energy per atom of the film. At finite T our results diverge from those reported recently by Taborek and Goodstein¹⁹ because this $T=0$ correction must be replaced by an unknown quantity.

Our ground-state energy for ^3He , $E_\Gamma = -11.73$ meV, also agrees very well with the experimental value -11.72 ± 0.2 meV obtained by Elgin *et al.*⁵ Note that Fig. 9 exhibits the strong dependence (linear at $T=0$ in the absence of band-structure effects²) of μ on coverage expected for a Fermi system.

Figures 10 and 11 give the specific heat for these coverages. The chief features of both curves are peaks at low temperature and large increases of C/Nk_B above unity at $T > 10$ K. The former arises because of the gap in $N(E)$, which causes a depression in C for $k_B T$ about half the gap energy.² The second feature occurs because of excitation of states of perpendicular motion. These represent the expected deviation from the simple two-dimensional view of He on graphite. In the latter picture, the form of the heat capacity is identical for both isotopes; C/Nk_B rises monotonically to unity, reaching 0.9 at $T = 3$ K and 0.5 K for $\theta = 1$ and 0.2 , respectively, for ^4He .²⁰

Because of the omission of the He-He interaction from our calculation, it is unrealistic to expect correspondence with experiment at low T . For $T > 3$ K, in contrast, the interactions contribute negligibly to C .¹⁷ Recent experimental results of Goodstein and coworkers²¹ show quite good agreement with our calculated heat capacities for T between 3 and 10 K. Discrepancies may con-

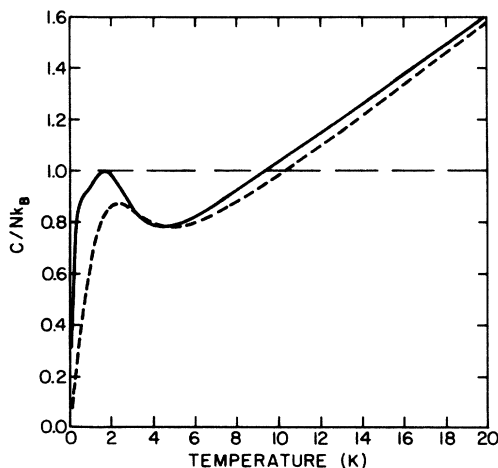


FIG. 10. ${}^4\text{He}$ specific heat for $\theta=0.2$ (full curve) and 1 (dashed curve).

ceivably be due to some inaccuracy in the very large desorption correction required to analyze the data.⁵ That procedure is tenuous because it neglects implicitly the higher- n bands. Obviously any conclusion concerning the origins of such discrepancies is speculative.

VI. SUMMARY AND CONCLUSIONS

We have presented an energy-band calculation for He atoms on graphite, focusing on two regimes of energy. At high energy, our results confirm the basic approach used to deduce the matrix elements of the corrugation function $V_{01}(z)$. That is, the splittings of the bound-state resonances correspond accurately to the value predicted by perturbation theory in terms of the matrix elements. The energy bands at low energy manifest the nonuniformity of $V(\vec{r})$ more dramatically. The zone-boundary gaps of Figs. 4 and 5 are comparable to the bandwidth. This contradicts, to some extent, the simple two-dimensional picture of He motion on graphite. Since that approach greatly facilitates calculations of film properties, these results are regrettable. Previous work^{12,13} on this system employed a less corrugated potential, but the latter is quite inconsistent with the scattering data.^{10,22} We emphasize that our conclusions are model independent since the present calculation is empirical. We reached the same conclusion previously¹⁰ by comparing with scattering data the predictions of various models for the He-C interaction. That analysis enabled us to pinpoint

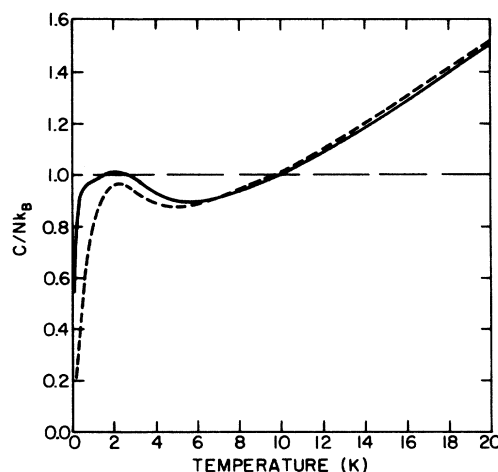


FIG. 11. Same as Fig. 10 for ${}^3\text{He}$.

the inadequacy of the assumption of an isotropic He-C interaction in earlier work.

Particularly impressive is the agreement between the band-structure results for the ground-state energy and its value determined from adsorption data. Credit should be directed toward the experimentalists,^{5,7,8} since the band-structure correction is only 1 percent of the total binding energy.

One prediction which can be tested by further experiment (e.g., thermodynamics or NMR) is the large effective-mass enhancement of Table I. It seems plausible, furthermore, that m^* should replace m in the calculations of film properties.¹⁷ The latter are not at present sufficiently accurate to test the prediction however.

We may summarize the present results by saying that the relatively corrugated potential obtained by CC is responsible for rather marked effects on the single-particle spectrum at low energy. We urge experimentalists to explore the regime of low coverage and temperature, especially on high-quality graphite substrates.

ACKNOWLEDGMENTS

We are indebted to the experimental groups at The Pennsylvania State University, the University of Genoa, and the California Institute of Technology for providing data prior to publication. Especially helpful have been discussions with D. R. Frankl, G. Boato, W. A. Steele, D. L. Goodstein, and J. Weare. This work was prepared for the United States Department of Energy under Contract No. DE-AC02-79ER10454.

- *Present address: Code 6877, Naval Research Laboratory, Washington, D.C. 20375.
- ¹W. A. Steele, *Interaction of Gases with Solid Surfaces* (Pergamon, Oxford, 1974).
- ²J. G. Dash, *Films on Solid Surfaces* (Academic, New York, 1975).
- ³K. Carneiro, W. D. Ellenson, L. Passell, J. P. McTague, and H. Taub, *Phys. Rev. Lett.* **37**, 1695 (1976).
- ⁴E. J. Derderian and W. A. Steele, *J. Chem. Phys.* **66**, 2831 (1977).
- ⁵R. L. Elgin and D. L. Goodstein, *Phys. Rev. A* **9**, 2657 (1974); R. L. Elgin, J. M. Greif, and D. L. Goodstein, *Phys. Rev. Lett.* **41**, 1723 (1978).
- ⁶M. Bretz, J. G. Dash, D. C. Hickernell, E. O. Mclean, and O. E. Vilches, *Phys. Rev. A* **8**, 1589 (1973).
- ⁷G. Derry, D. Wesner, W. E. Carlos, and D. R. Frankl, *Surf. Sci.* **87**, 629 (1979).
- ⁸G. Boato, P. Cantini, R. Tatarek, *Phys. Rev. Lett.* **40**, 887 (1978); G. Boato, P. Cantini, R. Tatarek, and G. P. Felcher, *Surf. Sci.* **80**, 518 (1979); G. Boato, P. Cantini, C. Guidi, R. Tatarek, and G. P. Felcher *Phys. Rev. B* **20**, 3957 (1979).
- ⁹W. E. Carlos and M. W. Cole, *Phys. Rev. Lett.* **43**, 697 (1979).
- ¹⁰W. E. Carlos and M. W. Cole, *Surf. Sci.* **91**, 339 (1980).
- ¹¹Models using a corrugated hard wall plus attraction have been considered by V. Celli, N. Garcia, and J. Hutchinson, *Surf. Sci.* **87**, 101 (1979), and N. Garcia, W. E. Carlos, M. W. Cole, and V. Celli, *Phys. Rev.*, in press.
- ¹²D. E. Hagen, A. D. Novaco, and F. J. Milford, in *Adsorption-Desorption Phenomena*, edited by F. Ricca (Academic, London, 1972), p. 99; E. Giamello, C. Pisani, F. Ricca, and C. Roetti, *Surf. Sci.* **49**, 401 (1975).
- ¹³H. Chow, *Surf. Sci.* **79**, 157 (1979).
- ¹⁴K. L. Wolfe and J. H. Weare, *Phys. Rev. Lett.* **41**, 715 (1978).
- ¹⁵See, e.g., N. W. Ashcroft and N. D. Mermin, *Solid State Physics* (Holt, Rinehart, and Winston, New York, 1976), Chap. 9.
- ¹⁶H. Chow, *Surf. Sci.* **62**, 487 (1977).
- ¹⁷G. Bonino, C. Pisani, F. Ricca, and C. Roetti, *Surf. Sci.* **50**, 379 (1975). These workers did include the effects of anisotropy in their potential but due to the choice of parameters still found a much less corrugated potential than in the current work.
- ¹⁸See, e.g., R. L. Siddon and M. Schick, *Phys. Rev. A* **9**, 907 (1974); M. D. Miller, C.-W. Woo, and C. E. Campbell, *ibid.* **6**, 1974 (1972).
- ¹⁹P. Taborok and D. Goodstein, *Rev. Sci. Instrum.* **50**, 227 (1979).
- ²⁰R. M. May, *Phys. Rev.* **135**, A1515 (1964).
- ²¹D. L. Goodstein, private communication.
- ²²Even within the framework of isotropic pair potentials, earlier parametrizations were inadequate. See W. E. Carlos and M. W. Cole, *Surf. Sci.* **77**, L173 (1978) and Garcia *et al.*, Ref. 11.